

Hollow Co₂P nanoflowers organized by nanorods for ultralong cycle-life supercapacitors

Ming Cheng^{a,b}, Hongsheng Fan^{a,b}, Yingying Xu^c, Rongming Wang^{c,*}, Xixiang Zhang^{b,*}

^a Department of Physics, Beihang University, Beijing 100191, P. R. China

^b King Abdullah University of Science and Technology (KAUST), Physical Science and Engineering Division (PSE), Thuwal 23955-6900, Saudi Arabia

^c Beijing Key Laboratory for Magneto-Photoelectrical Composite and Interface Science, School of Mathematics and Physics, University of Science and Technology Beijing, Beijing 100083, P. R. China

* Corresponding authors: rmwang@ustb.edu.cn, xixiang.zhang@kaust.edu.sa

The theoretical capacity value of Co₂P and Ni₂P

The formula used to calculate theoretical capacity: $C = n \times F / (V \times M)$, where n is the moles of charge transferred per mole of active material, F is Faraday's constant (96485.3383 C mol⁻¹), M is the molar mass of the active material, and V is the potential range.¹ For comparison, V is supposed to be 0.5 V for both samples here.

For Co₂P, $C_1 = (4 - \delta_1) \times 2601 \text{ F g}^{-1}$, ($0 < \delta_1 < 1$);^{2,3}

For Ni₂P, $C_1 = (3 - \delta_2) \times 2601 \text{ F g}^{-1}$, ($0 < \delta_2 < 1$);^{2,3}

So cobalt phosphides should have a higher theoretical capacity than nickel phosphides.

The details of the calculation methods

The electronic band structure of Co₂P is evaluated by the density functional theory calculations performed using CASTEP.⁴ The OTFG ultrasoft pseudo-potentials and generalized gradient approximation (GGA) with the Perdew-Burke-Ernzerhof (PBE) exchange-correlation functional are adopted. Plane-wave basis sets with the energy cutoff of 600 eV are used to expand the electronic wave-functions. The residual energy are less than 10⁻⁶ eV for each atom. A Γ center (9×13×7) Monkhorst-Pack grid of k points is used for the DOS calculations. Co₂P have the C₂₃ orthorhombic structure with the space group D_{2h}^{16} (Pnma). The lattice constants and atomic positional parameters of Co₂P are shown in below.³

| | a (nm) | b (nm) | c (nm) | | x | y | z |
|-------------------|--------|--------|--------|------------------|--------|--------|--------|
| Co ₂ P | 0.5646 | 0.3513 | 0.6608 | Co _I | 0.8560 | 0.2500 | 0.0647 |
| | | | | Co _{II} | 0.9685 | 0.2500 | 0.6657 |
| | | | | P | 0.2461 | 0.2500 | 0.1249 |

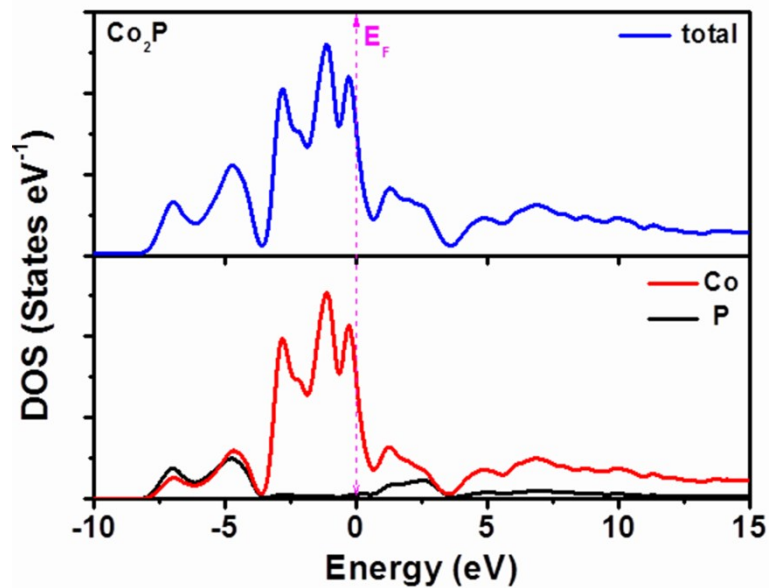


Fig. S1 Total densities of states and partial densities of states curves of Co₂P.

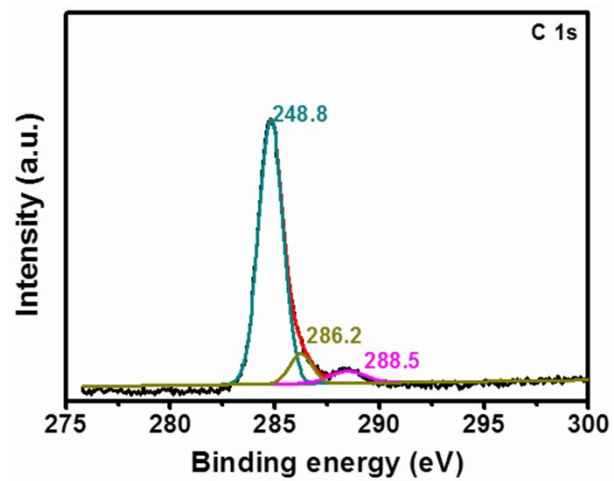


Fig. S2 High resolution XPS spectra of C 1s for Co₂P HNF.

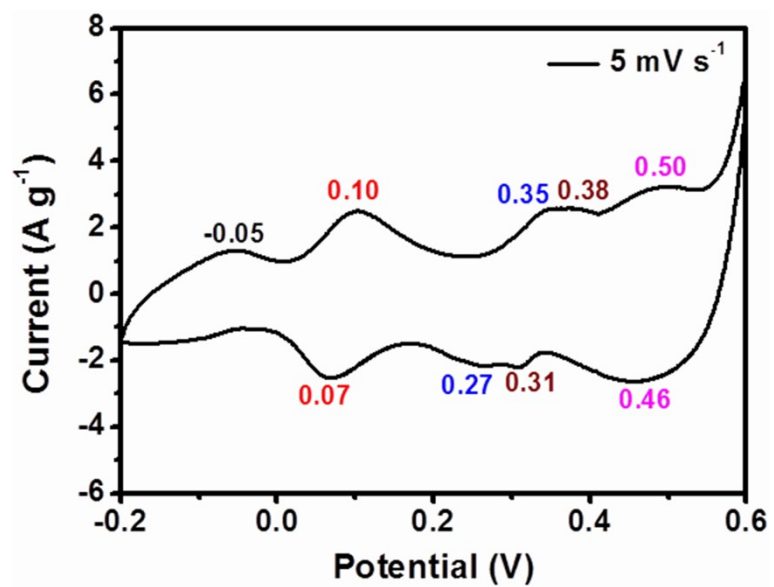


Fig. S3 CV curve of Co₂P HNF at a scan rate of 5 mV·s⁻¹.

Electrocatalytic Activity toward OER

OER activity was evaluated in a standard three-electrode cell with platinum foil as the counter electrode and Ag/AgCl (KCl saturated) as the reference electrode. To prepare the working electrode, 7.0 mg of Co₂P catalyst was dispersed in 2 mL of solution (1 mL of DI water, 0.88 mL of isopropanol and 0.12 mL of 5 wt.% Nafion solution) by ultrasonication. Then, 11 μ L of the catalyst suspension was carefully pipetted onto the glass carbon (GC) electrode surface with a diameter of 5 mm. The coated electrode was dried in air. The catalyst loading amount is 0.2 mg cm⁻² on the GC electrode. Potentials were referenced to a reversible hydrogen electrode (RHE): $E(\text{RHE}) = E(\text{Ag}/\text{AgCl}) + (0.1976 + 0.059 \text{ pH})$. Linear sweep voltammetry (LSV) was recorded in O₂-saturated 1.0 M KOH (pH = 13.62) at a scan rate of 5 mV s⁻¹ to obtain the polarization curves. The long-term stability tests were performed by continuous LSV scans at a sweep rate of 100 mV s⁻¹. The polarization curves were all corrected by 95% iR compensation. Cyclic voltammetry curves were conducted from 0.80 to 0.88 V (vs. RHE) without faradaic processes at different scan rates (5 to 12.5 mV/s). The I-t curve was measured under a fixed overpotential of 0.37 V.

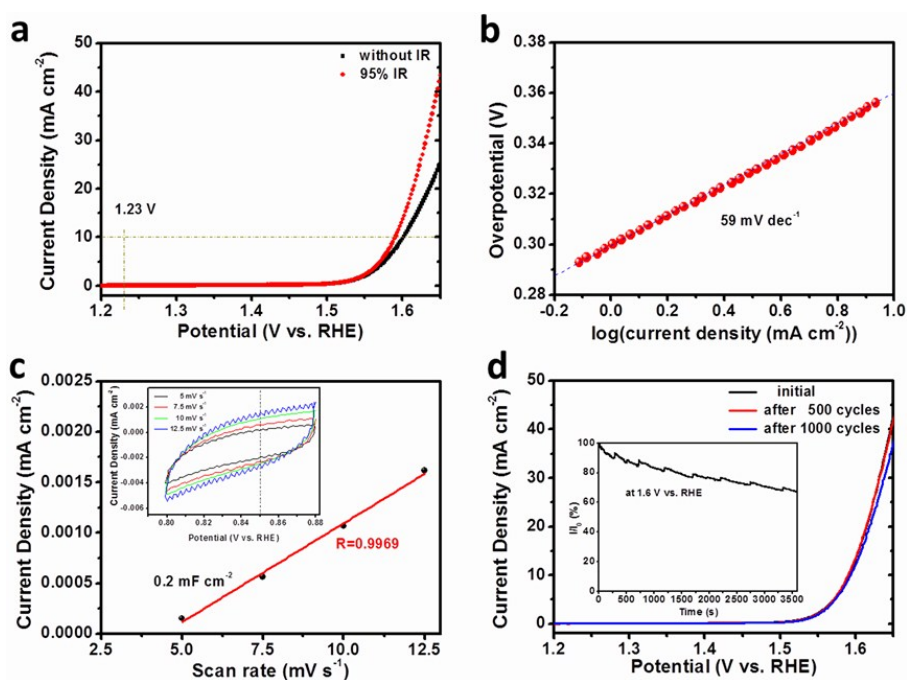
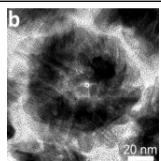
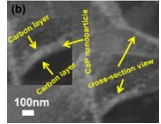
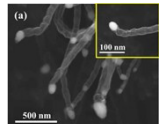
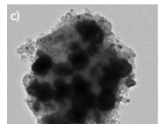
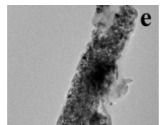
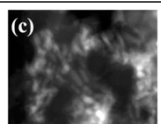

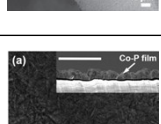
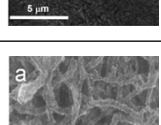
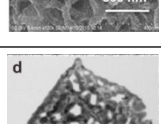
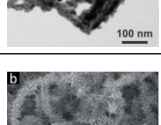


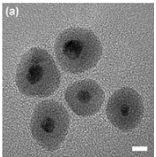
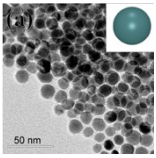
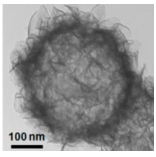
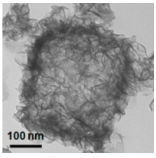
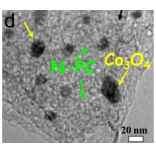
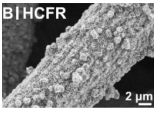
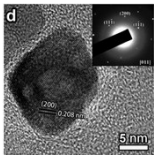
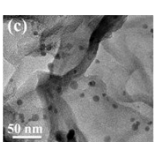
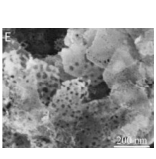
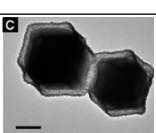
Fig. S4 Electrochemical performance of the OER catalysts in 1 M KOH: (a) The polarization curves of Co₂P HNF. (b) Tafel curves of Co₂P HNF. (c) Scan rate

dependence of the average apacitive currents at 0.85 V vs. RHE of Co₂P HNF. Inset is the cyclic voltammogram curves in a potential window without faradaic processes. (d) The stability of Co₂P HNF modified electrode before and after LSV testing for 500 and 1000 cycles, respectively. Inset is the current-time plot of Co₂P HNF electrode with a constant applied potential of 1.60 V vs. RHE.

The OER activities of Co₂P HNF were evaluated in a high pure O₂-saturated 1.0 M KOH solution using a standard three electrodes setup. As shown in Fig. S4a, Co₂P HNF affords a current density of 10 mA cm⁻² at 1.590 V (vs. RHE). The Tafel slope of Co₂P HNF, which is usually used to evaluate the efficiency of the catalytic reaction,⁵ is also determined to be 59 mV dec⁻¹ (Fig. S4b). Furthermore, the electrochemically active surface area of Co₂P HNF can be estimated from the electrochemical double-layer capacitances of the catalytic surface by measuring the CV curves in the potential range of 0.80 – 0.88 V (vs. RHE) without redox process (Fig. S4c).⁶ The capacitance of Co₂P HNF is measured to be 0.20 mF cm⁻². To assess the durability of Co₂P HNF electrocatalyst, continuous linear potential sweeps were conducted repeatedly on the electrode. Co₂P HNF exhibits inherent stability after 500 continuous cycles, and only a little anodic current loss is observed after 1000 cycles (Fig. S4d). The stability of the Co₂P HNF is further tested by using a chronoamperometric method at 1.60 V (vs. RHE), as shown in Fig. S4d. The OER activity retains 67% after 1 h, which could be ameliorated by improving adhesion of the powder to the electrode.⁷ The OER activity of Co₂P HNF is also compared with the previously previously transition metal compounds (Table S1). Though our prepared Co₂P HNF is not as good as the reported transition metal phosphide, it outperforms many reported transition metal oxides or hydroxides.

| Electrocatalysts | Morphology | Electrolyte | Loading (mg cm ⁻²) | η @10 mA cm ⁻² (mV) | Tafel slope (mV dec ⁻¹) | Ref. |
|-----------------------|---|-------------|--------------------------------|-------------------------------------|-------------------------------------|-----------|
| Co ₂ P HNF |  | 1.0 M KOH | 0.2 | 360 | 59 | This work |

| | | | | | | |
|---|---|------------|-------|-----|----|----|
| Sandwich-like CoP/C nanocomposites |  | 1.0 M KOH | 0.36 | 330 | 53 | 8 |
| Co₂P/CNT |  | 1.0 M KOH | 0.75 | 292 | 68 | 9 |
| Cu_{0.3}Co_{2.7}P/NC |  | 1.0 M KOH | 0.4 | 190 | 44 | 10 |
| CoP NR/C |  | 1.0 M KOH | 0.71 | 320 | 71 | 11 |
| CoP nanoparticles |  | 0.1 M KOH | 0.4 | 360 | 66 | 12 |
| CoP nanorod arrays on Ni foam |  | 1.0 M KOH | 6.2 | 290 | 65 | 13 |
| Co-P film |  | 1.0 M KOH | 1.0 | 345 | 47 | 14 |
| CoP/CNT |  | 0.1 M NaOH | 0.285 | 400 | 80 | 15 |
| Carbon coated Ni-P |  | 1.0 M KOH | 0.20 | 300 | 64 | 16 |
| FeP@CNT |  | 1.0 M KOH | 0.204 | 300 | 53 | 17 |

| | | | | | | |
|--|---|-----------|-------|-----|----|----|
| Au@Ni₁₂P₅ |  | 1.0 M KOH | 0.13 | 340 | 49 | 7 |
| Ni₁₂P₅ |  | 1.0 M KOH | 0.13 | 380 | 43 | |
| Hollow fluffy Co(OH)₂ |  | PH 14 KOH | 0.14 | 422 | 93 | 18 |
| Hollow fluffy Co₃O₄ |  | PH 14 KOH | 0.14 | 409 | 70 | |
| Co₃O₄/N-PC |  | 0.1 M KOH | 0.354 | 390 | 72 | 19 |
| NiCo LDH |  | 1.0 M KOH | 0.17 | 370 | 40 | 20 |
| Hollow CoO |  | 1.0 M KOH | 0.20 | 375 | 55 | 21 |
| PGE-CoO |  | 0.1 M KOH | 0.524 | 348 | 79 | 6 |
| Porous FeNi Oxides nanosheets |  | 1.0 M KOH | 0.254 | 213 | 32 | 22 |
| Co₃O₄/NiCo₂O₄ DSNCs |  | 1.0 M KOH | 1.0 | 340 | 88 | 5 |

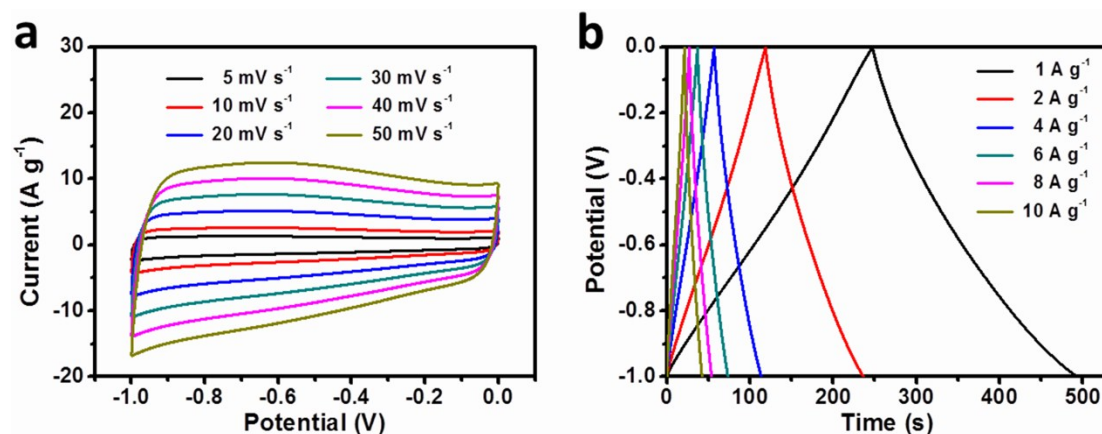


Fig. S5 (a) CV curves at different scan rates and (b) CP curves at different current densities of the active carbon (AC).

References

1. C. Zhou, Y. Zhang, Y. Li and J. Liu, *Nano Lett.*, 2013, **13**, 2078.
2. H. Liang, C. Xia, Q. Jiang, A. N. Gandi, U. Schwingenschlöggl and H. N. Alshareef, *Nano Energy*, 2017, **35**, 331.
3. S. Fujii, S. Ishida and S. Asano, *J. Physics F Metal Physics*, 1988, **18**, 971.
4. S. J. Clark, M. D. Segall, C. J. Pickard, P. J. Hasnip, M. J. Probert, K. Refson and M. C. Payne, *Zeitschrift Fur Kristallographie*, 2005, **220**, 567.
5. H. Hu, B. Guan, B. Xia and X. W. Lou, *J. Am. Chem. Soc.*, 2015, **137**, 5590.
6. Y. Zhao, B. Sun, X. Huang, H. Liu, D. Su, K. Sun and G. Wang, *J. Mater. Chem. A*, 2015, **3**, 5402.
7. Y. Xu, S. Duan, H. Li, M. Yang, S. Wang, X. Wang and R. Wang, *Nano Res.*, 2017, DOI:10.1007/s12274-017-1527-1.
8. Y. Bai, H. Zhang, Y. Feng, L. Fang and Y. Wang, *J. Mater. Chem. A*, 2016, **4**, 9072.
9. D. Das and K. K. Nanda, *Nano Energy*, 2016, **30**, 303.
10. J. Song, C. Zhu, B. Z. Xu, S. Fu, M. H. Engelhard, R. Ye, D. Du, S. P. Beckman and Y. Lin, *Adv. Energy Mater.*, 2017, **7**, 1601555.
11. J. Chang, Y. Xiao, M. Xiao, J. Ge, C. Liu and W. Xing, *ACS Catal.*, 2015, **5**, 6874.
12. J. Ryu, N. Jung, J. H. Jang, H.-J. Kim and S. J. Yoo, *ACS Catal.*, 2015, **5**, 4066.
13. Y.-P. Zhu, Y.-P. Liu, T.-Z. Ren and Z.-Y. Yuan, *Adv. Funct. Mater.*, 2015, **25**, 7337.
14. N. Jiang, B. You, M. Sheng and Y. Sun, *Angew. Chem. Int. Edit.* 2015, **54**, 6251.
15. C. C. Hou, S. Cao, W. F. Fu and Y. Chen, *ACS Appl. Mater. Inter.*, 2015, **7**, 28412.
16. X. Yu, Y. Feng, B. Guan, X. W. D. Lou and U. Paik, *Energy Environ. Sci.*, 2016, **9**, 1246.
17. Y. Yan, B. Zhao, S. C. Yi and X. Wang, *J. Mater. Chem. A*, 2016, **4**, 13005.
18. X. Zhou, X. Shen, Z. Xia, Z. Zhang, J. Li, Y. Ma and Y. Qu, *ACS Appl. Mater. Inter.*, 2015, **7**, 20322.
19. Y. Hou, J. Li, Z. Wen, S. Cui, C. Yuan and J. Chen, *Nano Energy*, 2015, **12**, 1.
20. H. Liang, F. Meng, M. Caban-Acevedo, L. Li, A. Forticaux, L. Xiu, Z. Wang and S. Jin, *Nano Lett.*, 2015, **15**, 1421.
21. M. Cheng, S. Duan, H. Fan and R. Wang, *CrystEngComm*, 2016, **18**, 6849.
22. X. Long, Z. Ma, H. Yu, X. Gao, X. Pan, X. Chen, S. Yang and Z. Yi, *J. Mater. Chem. A*, 2016, **4**.